

Temperature stability of the pentacene thin-film phase

Armin Moser, Jií Novák, Heinz-Georg Flesch, Tatjana Djuric, Oliver Werzer et al.

Citation: *Appl. Phys. Lett.* **99**, 221911 (2011); doi: 10.1063/1.3665188

View online: <http://dx.doi.org/10.1063/1.3665188>

View Table of Contents: <http://apl.aip.org/resource/1/APPLAB/v99/i22>

Published by the [American Institute of Physics](http://www.aip.org).

Related Articles

X-ray reciprocal space mapping of dislocation-mediated strain relaxation during InGaAs/GaAs(001) epitaxial growth

J. Appl. Phys. **110**, 113502 (2011)

Effect of metal-precursor gas ratios on AlInN/GaN structures for high efficiency ultraviolet photodiodes

J. Appl. Phys. **110**, 103523 (2011)

Temperature dependent optical properties of pentacene films on zinc oxide

Appl. Phys. Lett. **99**, 211102 (2011)

Epitaxial lateral overgrowth of InN by rf-plasma-assisted molecular-beam epitaxy

AIP Advances **1**, 042145 (2011)

Growth of GaN on Si(111): Surfaces and crystallinity of the epilayers and the transport behavior of GaN/Si heterojunctions

J. Appl. Phys. **110**, 093514 (2011)

Additional information on *Appl. Phys. Lett.*

Journal Homepage: <http://apl.aip.org/>

Journal Information: http://apl.aip.org/about/about_the_journal

Top downloads: http://apl.aip.org/features/most_downloaded

Information for Authors: <http://apl.aip.org/authors>

ADVERTISEMENT

The logo for AIP Advances features the text 'AIP Advances' in a blue and green font. Above the text is a decorative graphic of several orange and yellow circles of varying sizes, arranged in a curved path that suggests motion or a trail of particles.

Submit Now

Explore AIP's new
open-access journal

- Article-level metrics now available
- Join the conversation! Rate & comment on articles

Temperature stability of the pentacene thin-film phase

Armin Moser,^{1,a)} Jiří Novák,¹ Heinz-Georg Flesch,¹ Tatjana Djuric,¹ Oliver Werzer,¹ Anja Haase,² and Roland Resel^{1,a)}

¹Institute of Solid State Physics, Graz University of Technology, Austria

²Institute for Surface Technologies and Photonics, Joanneum Research Weiz, Austria

(Received 7 September 2011; accepted 9 November 2011; published online 1 December 2011)

This work presents the influence of temperatures above 300 K on the crystal structure and morphology of pentacene thin films. The thermal expansion of the unit cell and the relative amount of different phases are investigated via grazing incidence x-ray diffraction. Geometrical considerations about the specific molecular packing of the thin-film phase explain the anisotropic non-linear expansion. Furthermore, around 480 K, a phase transformation of the thin-film phase to the bulk phase is observed. In contrast, only a weak influence of the temperature on the height distribution of the thin-film phase crystallites is found. © 2011 American Institute of Physics. [doi:10.1063/1.3665188]

Pentacene is a material widely used in organic thin film transistor research where thin films with thicknesses of some tens of nanometers are relevant. Although there are several polymorphic phases of pentacene¹ typically only two of them are observed in thin films: the thin-film phase and Campbell phase.^{2–5} While the Campbell phase is a bulk equilibrium structure, the thin-film phase is a surface induced, metastable crystallographic phase, which is kinetically favored during the growth process.⁶ On weakly interacting substrates (e.g., silicon oxide), the crystallites of both phases are commonly oriented with the (001) lattice plane parallel to the substrate surface; i.e., the *a* and *b* unit cell vectors lie in the substrate surface plane and the long molecular axis (LMA) is nearly perpendicular onto the substrate surface. Atomic force microscopy (AFM) experiments commonly show terraced, dendritic islands with diameters of some microns.^{7,8}

Despite the large number of scientific publications on pentacene thin films, there are only two studies showing some influence of temperatures above 300 K.^{9,10} Moreover, they are more focused on device performance than on crystallographic properties. To fill this gap, we have thoroughly investigated the crystallographic properties as well as the morphology via specular and grazing incidence x-ray diffraction experiments at temperatures ranging from 300 K up to desorption of the film at around 500 K.

Pentacene thin films with a nominal thickness of 50 nm have been physical vapor deposited onto thermally oxidized silicon wafers at a base pressure of 1×10^{-5} mbar; the substrate was kept at room temperature. For the starting 5 nm, a rate of 0.1 nm/min while for the remaining ones, a rate of 0.6 nm/min was used. AFM experiments were performed on a commercial Dimension 3100 by Veeco with standard silicon tips in tapping mode at ambient conditions and reveal the usually observed morphology. Grazing incidence and specular x-ray diffraction experiments have been performed at the ID10B beamline of the European Synchrotron Radiation Facility. For a wavelength and goniometer independent

representation of the data, the components of the scattering vector \vec{q} in the surface reference frame¹¹ are used as coordinates. For temperature control and creation of a helium inert atmosphere, a Domed Hot Stage 900 (Ref. 12) from Anton Paar Ltd. was used. To account for the thermal expansion of the heating stage, it was necessary to align the samples at each temperature step.

In the measured reciprocal space maps (RSM), diffraction peaks of the thin-film phase and Campbell phase have been observed. The positions of the Bragg peaks have been used to calculate the unit cell parameters at different temperatures. For the thin-film phase, clear thermal shifts of the lattice parameters are observed (depicted in Fig. 1). The

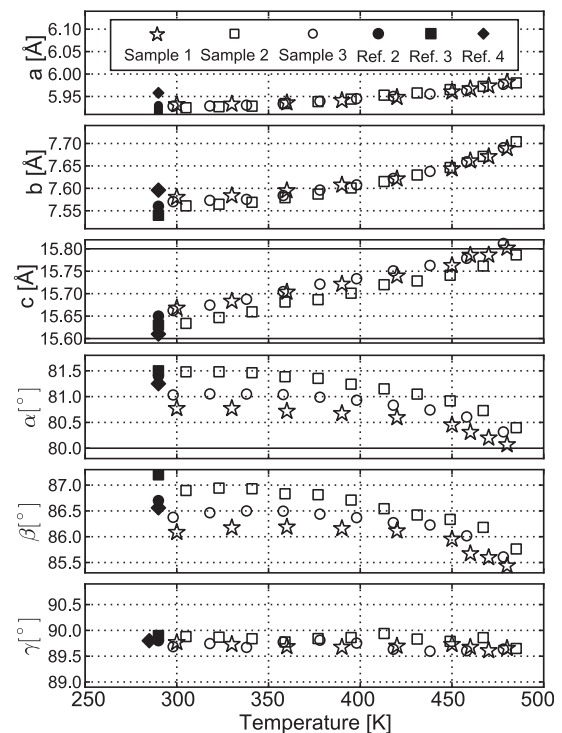


FIG. 1. Lattice constants of the pentacene thin-film phase as function of the temperature obtained from three independent diffraction experiments (empty symbols). The literature values at room temperature are given additionally (filled symbols).

^{a)}Author to whom correspondence should be addressed. Electronic addresses: armin.moser@tugraz.at and roland.resel@tugraz.at.

temperature dependence of the lattice constants a and b is non-linear, in contrast to that of c . Furthermore, the expansion of b ($\approx 0.12 \text{ \AA}$) is approximately twice that of a ($\approx 0.05 \text{ \AA}$). This 2:1 ratio of the expansion was also found for the Holmes phase^{1,13} under high pressure.¹⁴ This observation is typical for the herringbone packing motive and explained by geometrical considerations taking the van der Waals shape of the molecules into account.¹⁴ Also, the non linearity of the in-plane expansion is caused by the distinct packing of the molecules. The molecules are nearly perpendicular onto the (001) plane, and hence the projection of their van der Waals shape to the (001) plane is elliptical. Upon heating, librations of the rigid molecules around their LMA play an important role.¹⁵ To avoid overlapping caused by the librations, the molecules have to shift (non linearly) into a and b direction. In contrast, the lattice constant c is nearly parallel to the LMA and the expansion is, therefore, dominated by translations of the whole molecule. Hence, a more linear expansion into this direction is observed. An influence of the substrate is ruled out because the linear expansion coefficient ($\frac{1}{L(T_0)} \frac{\Delta L}{\Delta T}$) of amorphous silicon oxide ($\approx 0.5 \times 10^{-6} \text{ K}^{-1}$)¹⁶ is two orders of magnitude smaller than the one observed for pentacene ($\approx 1 \times 10^{-4} \text{ K}^{-1}$). In contrast to the thin-film phase, no reliable expansion curves could be obtained for the Campbell phase as only five peaks have been observed.

While the unit cell expansion was determined from the Bragg peak positions, their intensities were analyzed to investigate quantitative changes of the observed phases during temperature treatment. To perform this analysis, the intensities in the RSM have been summed along the q_z direction. From the resulting line scans (see Fig. 2), the total integrated intensities per phase have been extracted and depicted in Fig. 3. At room temperature, diffraction features from both phases are present, however upon heating, the Campbell phase intensity starts to decrease while the thin-film phase intensity remains constant or even increases slightly. Between 380 K and 450 K, no intensity from the Campbell phase is observed, but above 450 K, it reappears and reaches a maximum intensity at around 480 K. Above this temperature, finally both phases start to desorb and reach zero intensity around 500 K. Contrary, in the specular diffraction data (Fig. 4), the peak of the Campbell phase is only observed up to 360 K and the recurrence at 480 K cannot be recognized.

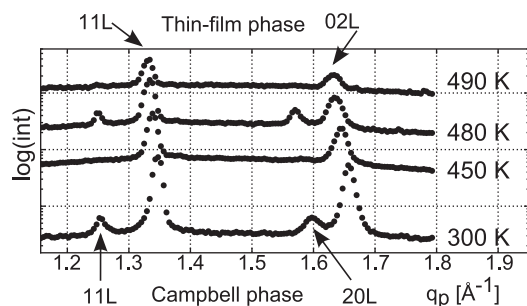


FIG. 2. Diffraction patterns at different temperatures as function of the scattering vector component parallel to the substrate surface (q_p). The patterns were obtained by integrating Bragg peak series observed in a reciprocal space map along q_z ranging from 0 to 1.0 \AA^{-1} . The observed peaks can be assigned to the thin-film phase (indicated above) and the Campbell phase (indicated below).

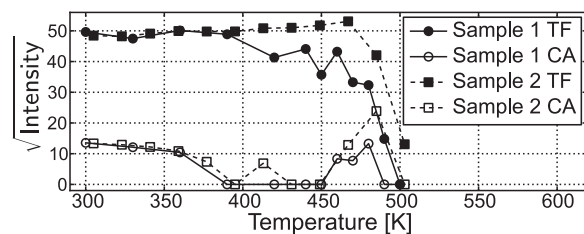


FIG. 3. Sum of Bragg peak intensities for the thin-film (TF) and for the Campbell (CA) phase which have been extracted from the in-plane scattering patterns. The data for two independent samples are presented.

At low temperatures, these observations show the vanishing of the Campbell phase while around 480 K, a transformation from the thin-film phase to the Campbell phase is observed. When comparing the specular and in-plane data around 480 K, it becomes obvious that the reformed Campbell phase crystallites have only a small vertical scattering volume but laterally a large one. In perfect agreement with our findings, the AFM images of Ji *et al.*⁹ show thin elongated islands crystallizing on top of the film.

To gain more details about the phase changes and the morphology of the thin films, the specular diffraction data have been further analyzed. For this purpose, the height of each island is expressed in terms of the number of crystallographic layers N_i . Then, the diffraction peak from one phase is described by a weighted sum of the interference functions from individual islands of specific height (Eq. (1)). The weights are determined by the island height distribution which has been chosen Gaussian in the present case (Eq. (2)).¹⁷ Furthermore to account for the two crystallographic phases, their diffraction is calculated separately and then added. To perform global optimization, the described model was implemented in the software package GenX.¹⁸

$$I = \sum_{N_i=N_{min}}^{N_{max}} w_{N_i} \cdot \frac{\sin^2(N_i/2 \cdot qd_{001})}{\sin^2(1/2 \cdot qd_{001})}, \quad (1)$$

$$w_{N_i} = \frac{1}{\sqrt{(2\pi)\Delta N^2}} \exp\left(-\frac{(N_i - N)^2}{\Delta N^2}\right). \quad (2)$$

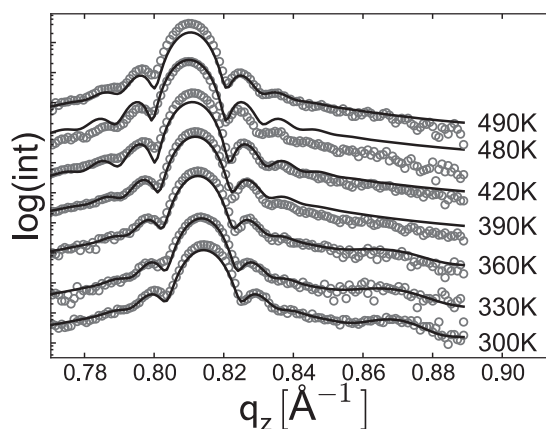


FIG. 4. Specular diffraction around the 002 Bragg peak of the thin-film phase ($q_z \approx 0.81 \text{ \AA}^{-1}$) and of the Campbell phase ($q_z \approx 0.87 \text{ \AA}^{-1}$) at different temperatures. The symbols indicate the experimental data while the lines correspond to fits using the model defined in Eqs. (1) and (2).

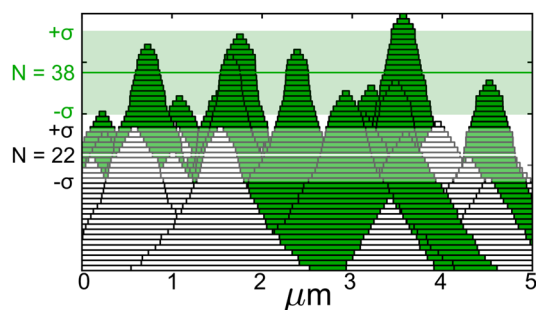


FIG. 5. (Color online) Sketch of the Gaussian height distribution of the pentacene crystallites at 360 K. The filled islands show the thin-film phase while the empty ones correspond to the Campbell phase. The mean island heights (N) are indicated by a horizontal colored and white line. The standard deviation ($\pm\sigma$) areas are shaded. The parameters have been obtained from the corresponding fit of the specular data shown in Fig. 4.

For the thin-film phase, this analysis revealed, within the experimental precision, a constant mean island height ($N \approx 38$) and standard deviation ($\Delta N \approx 7$). The thickness of the Campbell phase was found to be $N \approx 26$ with $\Delta N \approx 5$ at room temperature and to decrease to $N \approx 22$ at 330 K and 360 K. A sketch of the height distribution at 360 K is shown in Fig. 5. Please note that in the RSM, the lateral width of the diffraction peaks is dominated by the resolution function of the apparatus and hence no lateral crystal size can be determined. Therefore, the lateral widths for the above sketch have been chosen to resemble the island size typically observed in AFM images. It is also noted that below 420 K, no broadening of the peaks due to temperature is observed.¹⁹

The morphological information obtained proves that after the deposition process, the thin-film phase crystallites are larger than the Campbell phase crystallites. Therefore, it is suggested that upon heating—in analogy to Ostwald ripening—the thin-film phase crystallites grow on the expense of the Campbell phase. This is confirmed by the slight increase of the thin-film phase intensity in Fig. 3. In contrast around 480 K, it is supposed that the metastable thin-film phase transforms into the more stable Campbell phase. In view of the used model, the constant height distribution hints that during the phase transition, some of the thin-film phase crystallites transform completely into the Campbell phase. This behavior is similar to powders or single crystals where around 470 K, a phase transition from the Holmes phase to the Campbell phase was found.²⁰

In summary, we have found that the thermal expansion of the thin-film phase is independent from the substrate and its non-linearity caused by the distinct packing of the molecules. Between 300 K and 400 K, the initially observed

Campbell phase vanishes while at higher temperatures, a phase transition from the metastable thin-film phase to the more stable Campbell phase was found. The morphological information obtained indicates that some crystallites change their crystal structure completely while the largest part of the crystallites stays unchanged. These findings encourage molecular dynamics calculations^{21,22} to further study the details of the phase transformation from the thin-film to the Campbell phase around 480 K.

We thank the European Synchrotron Radiation Facility and F. Zontone as well as O. Konovalov for assistance. This work was supported by the Austrian Science Fund (FWF):[P21094].

- ¹C. C. Mattheus, A. B. Dros, J. Baas, A. Meetsma, J. L. de Boer, and T. T. M. Palstra, *Acta Crystallogr.* **57**, 939 (2001).
- ²H. Yoshida and N. Sato, *Phys. Rev. B* **77**, 235205 (2008).
- ³D. Nabok, P. Puschnig, C. Ambrosch-Draxl, O. Werzer, R. Resel, and D.-M. Smilgies, *Phys. Rev. B* **76**, 235322 (2007).
- ⁴S. Schiefer, M. Huth, A. Dobrinevski, and B. Nickel, *J. Am. Chem. Soc.* **129**, 10316 (2007).
- ⁵R. B. Campbell, J. M. Robertson, and J. Trotter, *Acta Crystallogr.* **15**, 289 (1962).
- ⁶C. D. Dimitrakopoulos, A. R. Brown, and A. Pomp, *J. Appl. Phys.* **80**, 2501 (1996).
- ⁷F. Zhang, Z. Xu, X. Liu, S. Zhao, L. Lu, Y. Wang, and X. Xu, *Superlattices Microstruct.* **45**, 612 (2009).
- ⁸U. Haas, A. Haase, H. Maresch, B. Stadlober, and G. Leising, in *4th IEEE International Conference on Polymers and Adhesives in Microelectronics and Photonics, 2004. POLYTRONIC 2004* (IEEE, Piscataway, NJ, 2004), pp. 219–224.
- ⁹T. Ji, S. Jung, and V. K. Varadan, *Org. Electron.* **9**, 895 (2008).
- ¹⁰K. Fukuda, T. Sekitani, and T. Someya, *Appl. Phys. Lett.* **95**, 023302 (2009).
- ¹¹A. Moser, O. Werzer, H.-G. Fleisch, M. Koini, D.-M. Smilgies, D. Nabok, P. Puschnig, C. Ambrosch-Draxl, M. Schiek, H.-G. Rubahn et al., *Eur. Phys. J. Spec. Top.* **167**, 59 (2009).
- ¹²R. Resel, E. Tamas, B. Sonderegger, P. Hofbauer, and J. Keckes, *J. Appl. Crystallogr.* **36**, 80 (2003).
- ¹³D. Holmes, S. Kumaraswamy, A. J. Matzger, and K. P. C. Vollhardt, *Chem.-Eur. J.* **5**, 3399 (1999).
- ¹⁴M. Oehzelt, A. Eichholzer, R. Resel, G. Heimel, E. Venuti, and R. G. D. Valle, *Phys. Rev. B* **74**, 104103 (2006).
- ¹⁵S. Haas, B. Batlogg, C. Besnard, M. Schiltz, C. Kloc, and T. Siegrist, *Phys. Rev. B* **76**, 205203 (2007).
- ¹⁶B. El-Kareh, *Fundamentals of Semiconductor Processing Technologies* (Kluwer Academic Publishers, Dordrecht, 1994).
- ¹⁷A. Nefedov, A. Abromeit, C. Morawe, and A. Stierle, *J. Phys.: Condensed Matter* **10**, 717 (1998).
- ¹⁸M. Björck and G. Andersson, *J. Appl. Crystallogr.* **40**, 1174 (2007).
- ¹⁹See supplementary material at <http://dx.doi.org/10.1063/1.3665188> for reciprocal space maps at 300 K and 360 K as well as in-plane peak widths as function of temperature.
- ²⁰T. Siegrist, C. Besnard, S. Haas, M. Schiltz, P. Pattison, D. Chernyshov, B. Batlogg, and C. Kloc, *Adv. Mater.* **19**, 2079 (2007).
- ²¹M. Yoneya, M. Kawasaki, and M. Ando, *J. Mater. Chem.* **20**, 10397 (2010).
- ²²A. Pizzirusso, M. Savini, L. Muccioli, and C. Zannoni, *J. Mater. Chem.* **21**, 125 (2011).